Coexistence between massive MIMO and radar communications: performance analysis

Elfiatoure, M., Ngo, H. Q., & Matthaiou, M. (2023). Coexistence between massive MIMO and radar communications: performance analysis. *Journal of Communications and Information Networks*, *8*(1), 37-47. https://doi.org/10.23919/jcin.2023.10087246

Published in:
Journal of Communications and Information Networks

Document Version:
Peer reviewed version

Queen's University Belfast - Research Portal:
Link to publication record in Queen's University Belfast Research Portal

Coexistence Between Massive MIMO and MIMO Radar

Mohamed Elfiatoure, Hien Quoc Ngo and Michail Matthaiou

***Abstract*— In the field of beyond-5G and 6G wireless communication systems, one trend that is gaining traction is investigating systems that perform both communication and sensing simultaneously. To enable the operation of these two systems with minimal mutual interference, we consider the coexistence of a massive multiple-input multiple-output (mMIMO) downlink and a multiple-input multiple-output (MIMO) radar. Unlike conventional methods in which radar and cellular systems work together. By using more antennas at the base station (BS), we demonstrate that massive MIMO can be improved while keeping radar interference at the same level. In addition, we can avoid interference from the massive MIMO system to the radar system with no compromise in performance if we use a large number of antennas at the BS and make the transmit power inversely proportional to the number of antennas. Furthermore, we formulate and solve a power allocation problem to maximize detection probability for MIMO radar. Finally, simulation results confirm the validity of our theoretical analysis and demonstrate that increasing the number of antennas for the BS and radar can effectively eliminate mutual interference.**

***Keywords*—Massive MIMO downlink, radar-communication coexistence, spectrum sharing.**

I. Introduction

With the rapid development of wireless communication systems such as the fifth generation (5G) networks and beyond, higher data rates and higher quality of service (QoS) are being aimed at, Massive multiple-input multiple-output (mMIMO) wireless communication systems utilize a large number of antennas at the communication base station compared to the number of users served. It has become an essential technology for the 5G wireless communications systems. With advances in mMIMO technology, 5G has the capacity to support high-definition video streaming and ultrafast broadband as well as other data-hungry applications. [1] [2] [3] [4]. Despite the exponential growth of wireless communication services and devices, the frequency spectrum is becoming increasingly congested due to the towering proliferation of connected devices and services. It has been reported that by 2030, the number of connected devices will exceed 29 billion [5]. Due to the rapid increase in applications using radio frequency spectrum, spectral congestion has increased and electromagnetic spectrum resources are becoming limited [6] [7] [8]. The radar and communication coexistence system has attracted extensive research attention because the spectrum sharing technique is the best solution to spectral congestion problems [9] [10] [11]. As a part of its proposed sharing of 150 MHz of 3.5 GHz spectrum with communication applications, the Federal Communications Commission (FCC) has proposed the sharing of 150 MHz of 3.5 GHz spectrum previously assigned to radar applications [12] [13]. For this reason, the radar bands are an excellent choice to be shared with communication systems due to the extensive spectrum available at radar frequencies, where the frequencies below 10GHz, the S-band (2-4GHz) and C-band are used for various radar applications [7] [14] . Due to this, the increasing demand for wireless communication systems and radar to share radio frequency bandwidth due to the urgent need for fast telecommunications and to address the scarcity of radio frequency bandwidth, where Spectrum sharing between communication and sensing systems offers a promising solution to elimination of spectrum congestion problem. Due to this, both academia and industry have shown considerable interest in spectrum sharing [15] [6] [16]. The past decade has seen Multi-input, multiple-output (MIMO) communication systems have attracted considerable attention in radar, which involves using multiple transmitters and multiple receivers. In contrast to traditional phased array radars, MIMO radars transmit multiple linearly independent probing signals. Moreover, the ability to identify parameters (location, distance, and

[0]********** ********.

Firstname1 Lastname1, Firstname2 Lastname2. Address1, City1 zipcode1, Country1 (e-mail: email1; email2).

Firstname1 Lastname1. Address2, City2 zipcode2, Country2 (e-mail: email1).

Firstname2 Lastname2. Address3, City3 zipcode3, Country3 (e-mail: email2).

speed of targets) as well as improved flexibility for transmitting beam pattern design is achieved through adaptive arrays for target detection, identifying parameters (location, distance, and speed of targets). [17] [18] [19]. Radar and communication spectrum sharing research is still in its infancy and therefore merits more extensive and comprehensive studies. In this article, we discuss some of the more noteworthy and related studies in the literature. Among the relevant works in this space, we have identified the following, the authors of [20] studied the coexistence of a rotating radar and a cellular communication system, during this scenario, the mainlobe of the radar array rotates periodically in search of potential targets. Therefore, BS is only allowed to transmit when they are in sidelobes. It also analyzes the communication performance in terms of downlink data rate based on the minimum distance between the two systems given the tolerable SINR level. Even though this approach is easy to implement in real-world scenarios, it does not share the same spectrum. Due to the radar occupying frequency and space resources, a communications system cannot function in this case [7]. In [21] [22], the approach has been adopted for the coexistence of MIMO radar and cellular, to avoid the interference effects on radar from the communication system, the transmitted power has been controlled by the base station while guaranteeing the receive signal interference noise ratio (SINR) level of downlink users. The study in [23] focused on improving the probability of detection by robust beamforming for MIMO radar while guaranteeing a satisfactory received SINR downlink for each user. A similar approach has been adopted in [24], who developed a Software-Defined Radio (SDR) based cognitive MIMO radar prototype using Universal Software Radio Peripheral (USRP) devices that coexist with LTE links. both studies focused on only the interference from the BS to the received radar without paying much attention to the radar's interference effects on the base station and users. According to [25] and [26], they introduced new method concept of reconfigurable intelligent surfaces (RISs) aimed at improving the coexistence and reducing mutual interference between radar and communication systems. For coexisting massive MIMO and MIMO radar in a recent study [27], the uplink was considered only, ignoring downlink communication and detection probability. The study also examined how radar interference affects communication systems on the uplink, while [28] focused on the worst-case interference on radar performance during the downlink, while paying no attention to the spectral efficiency and throughput of the cellular downlink. While the above mentioned studies concern, in particular, interference mitigation in coexistence with MIMO radar and communications, have mostly focused on interference from one side; With a limited number of antennas at the radar and BS. Both [29] and [23] generally focused on MIMO radar in order to maximize the probability of detection while guaranteeing a communication rate at the communication receive side. By utilizing precoding on both the radar and the communication system antennas, the author of [11] formulated the optimization problem to maximize radar signal-to-interference-plus-noise ratio (SINR) while enabling communication to meet its operational purpose. In [30], an optimization technique based on the Alternating Direction Method Of Multipliers (ADMM) for solving optimization problems has been developed in order to minimize the Cramér-Rao bound (CRB) for radar target estimation in the presence of interference from the communication system. It is discussed in paper [21] how beamforming at a base station can be optimized to minimize interference with nearby radars depending on transmission power and SINR, whereas [31] describes how beamforming on a ship-borne radar can be optimized to avoid interference with nearby cellular networks. It is important to emphasize that precoding techniques require the knowledge of the interfering channel either at the radar or at the communication base station [10]. It is quite common in the above works to assume imperfect channel state information (CSI). In [11], the information exchange is conducted between radar and communication systems via the control centre which connects both systems. Nevertheless, the control centre introduces considerable complexity into the system design and thus is difficult to implement in practice. According to [31], the MIMO radar has to estimate a channel from the pilot signals it receives from the BS, which requires additional computational resources. Aside from that, since the communication system takes advantage of the radar's spectrum, the performance of the radar is of primary concern, which means allocating radar resources to target detection rather than CSI.

The coexistence of radar and communications systems within acceptable performance has been extensively studied, but it has been difficult to get clear insights into how unaltered radar and communication systems affect each other in terms of imperfect channel state information for communication system. The assumption of perfect CSI is, however, an ideal one. In real-world systems, CSI should be estimated using training sequences or pilots. Channel estimation errors are inevitable due to the limited length of training sequences and the time-varying nature of wireless channels. For practical designs, it is important to consider the performance with imperfect CSI. An analysis of performance with imperfect CSI

is presented in this work. ***The coexistence of both technologies can improve wireless communication and radar performance, but it can also introduce mutual interference.***

[10] [11]

In this study, we analyze the performance of massive MIMO communication and MIMO radar for Maximum-ratio transmission (MR), Zero Forcing (ZF), and Protective Zero Forcing (PZF) with imperfect channel statistics. As a result of the recent developments in massive MIMO communications, we intend to investigate the potential benefits of coexisting massive MIMO with MIMO radar in order to mitigate the mutual interference from both technologies.

The specific contributions of our paper can be summarized as follows

- We analyze the system performance in the asymptotic regime under imperfect channel state information (CSI), where the number of BS antennas (where M is the number of BS antennas) goes to infinity. We demonstrate that the performance of the massive MIMO system can be improved by adding more antennas to the BS, while the interference to the radar system remains the same. Furthermore, by using large M and reducing transmit power by M times at the same time, we can avoid interference with radars and maintain a satisfactory quality of service for massive MIMO systems.
- We formulated and solved a power allocation problem to maximize the probability of detection for MIMO radar for both precoding MR, ZF and PZF under imperfect CSI. our proposed power allocation achieves up to $**\%$ detection probability gain over the non-optimized scenario.
- It is demonstrated in the numerical results that by increasing the antennas at both the BS and radar, target detection performance and spectral efficiency for users are improved. When the environmental conditions are harsh, for example when SNR is low, the improvement is even more noticeable. In addition, the effectiveness of radar is examined in relation to communications.

Notations: We denote vectors and matrices by lower-case boldface symbols and upper-case boldface symbols, respectively; $\mathbb{E}\{\cdot\}$ denotes the statistical expectation, $\|\cdot\|$ denotes the l_2 norm, $\mathrm{tr}(\cdot)$ denotes the matrix trace, $(\cdot)^H$ denotes the Hermitian transpose, $(\cdot)^\dagger$ denotes conjugate transpose, $(\cdot)^T$ denotes the matrix transpose, while $\mathbf{I}_M$ denotes an $M \times M$ identity matrix. Moreover, $\mathcal{CN}(0, \mathbf{C})$ denotes a circularly symmetric complex Gaussian vector with zero-mean and covariance matrix $\mathbf{C}$, $Q_n(.,.)$ denotes the Marcum Q-function of order n, whilst $I_{(n)}(x)$ denotes the modified Bessel function of the first kind and n-th order.

The rest of this paper is organized as follows. Section II defines the system model for the downlink Massive MIMO communication system coexists with a MIMO radar system on the same time-frequency resource. Next, Section III performance analysis. Then, Section IV problem formulation. Section V evaluates the system performance by using numerical results. Finally, the conclusion is drawn in Section VI.

II. System Model

We consider a time division duplex (TDD) downlink massive MIMO communication system coexists with a MIMO radar system on the same time-frequency resource. An array of M-antenna BS serves K single-antenna users $(M > K)$. The basic structure of the model is illustrated in Fig. 1, where:

- $\mathbf{g}_k \in \mathbb{C}^{M\times 1}$ is the channel vector response between the BS and the k-th user. The channel $\mathbf{g}_k$ is modeled as follows:
$$\mathbf{g}_k = {\beta_k}^{1/2}\mathbf{z}_k, \tag{1}$$
where $\mathbf{z}_k$ represents the small-scale fading, assuming to include independent and identically distributed (i.i.d.) random variables, i.e., $\mathbf{z}_k \sim \mathcal{CN}(0, \mathbf{I}_M)$, while β_k represents the large-scale fading.
- $\mathbf{R} \in \mathbb{C}^{N\times M}$ represents the interference channel matrix from the BS to the radar receiver, whose elements are i.i.d. $\sim \mathcal{CN}(0, \beta_{br})$, where β_{br} is the corresponding large-scale fading coefficient.
- $\mathbf{f}_k \in \mathbb{C}^{N\times 1}$ is the interference channel from the radar transmitter to the k-th user. Denote by $\mathbf{F} = [\mathbf{f}_1 \dots \mathbf{f}_K] \in \mathbb{C}^{N\times K}$ the corresponding channel matrix from the radar transmitter to all K users. We assume that $\mathbf{f}_k \sim \mathcal{CN}\left(0, \bar{\beta}_k \mathbf{I}_N\right)$, where $\bar{\beta}_k$ represents the large-scale fading.

In the following sub-sections, we provide details on the architecture of the two systems.

A. MIMO Radar

Consider MIMO radar system equipped with N_t transmitting antennas and N_r receiving antennas that is detecting targets located in the far field. we henceforth assume that $N_t = N_r = N$. The MIMO radar transmitter transmits probing signals to the target. Let $\mathbf{s} \in \mathbb{C}^{N_t\times 1}$, where $\mathbb{E}\left\{\mathbf{s}\mathbf{s}^H\right\} = \mathbf{I}_N$, be the radar transmit waveform. Assuming the MIMO radar-to-target channel is line-of-sight (LoS). Then, the reflected signal (echo from the

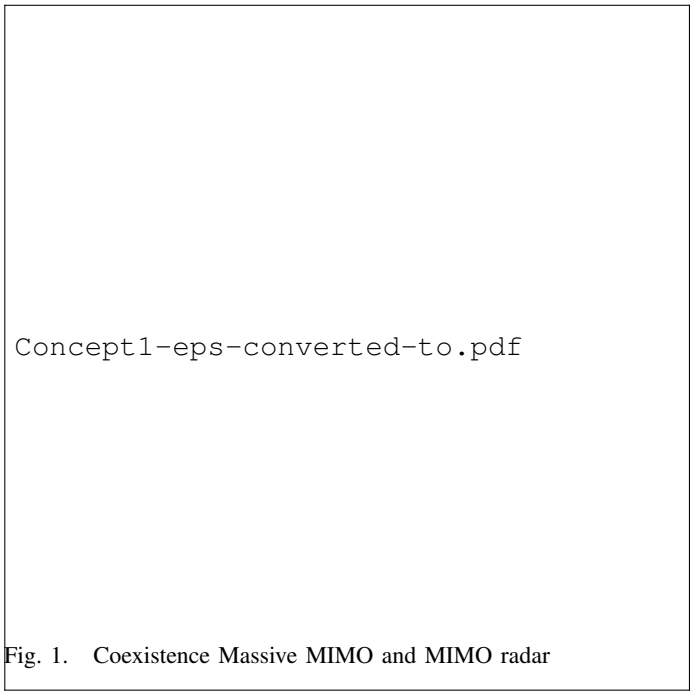

Fig. 1. Coexistence Massive MIMO and MIMO radar

target) from one point-like target to the radar receiver $\mathbf{y}^R$. The desired signal (echo from the target) is combined with interference from BS, as described below:

$$\mathbf{y}^R = \underbrace{\alpha\sqrt{P_R}\mathbf{A}(\theta)\mathbf{s}(\mathbf{t}-\tau)\mathbf{e}^{\mathrm{j}\omega\mathbf{t}}}_{\text{desired signal}} + \underbrace{\mathbf{R}^T\mathbf{x}}_{\text{interference from BS}} + \mathbf{w}, t \in [0,T], \quad (2)$$

where α, P_R, $\mathbf{x}$, $\mathbf{w} \sim \mathcal{CN}\left(0, \sigma_R^2\mathbf{I}_N\right)$, τ, ω and θ denote the complex path loss of the radar-target-radar path, the transmitted power for radar, the signal transmitted from the BS, the noise at the radar receiver, the time delay due to the target position with respect to the radar, Doppler shift as a result of velocity and position of the target and the azimuth angle of the target, respectively. Hence, $\mathbf{A}(\theta) = \mathbf{A}_R(\theta)\ \mathbf{A}_T^T(\theta)$, where $\mathbf{A}_R(\theta)$ and $\mathbf{A}_T^T(\theta)$ represent the transmit and receive steering vectors of radar antenna array respectively, where [23] [32]

$$\mathbf{A}_R(\theta) = \left[1, e^{-j\frac{2\pi d}{\lambda}\sin(\theta)}, \ldots, e^{-j\frac{2\pi d}{\lambda}(N_r-1)\sin(\theta)}\right]^T, \quad (3)$$

$$\mathbf{A}_T(\theta) = \left[1, e^{-j\frac{2\pi d}{\lambda}\sin(\theta)}, \ldots, e^{-j\frac{2\pi d}{\lambda}(N_t-1)\sin(\theta)}\right]^T, \quad (4)$$

where, d and λ represent inter-antenna spacing and the signal wavelength, where $d = \lambda/2$.

B. Massive MIMO Communication

Our focus here is on data transmission over the downlink with TDD operation. Based on the channel estimations obtained in the uplink training phase, maximum transmission (MR), zero forcing (ZF) or protective zero forcing (PZF) processing is applied to send data in the same time-frequency band to all users.

1) Uplink training: Let τ_{p} be the number of symbols per coherence interval used entirely for uplink pilots. All users simultaneously transmit pilot sequences of length τ_{p} symbols. The pilot sequences of K users are pairwisely orthogonal. Therefore, it is required that $\tau_{\mathrm{p}} \geq K$. The actual channel can be represented as

$$\mathbf{g}_k = \hat{\mathbf{g}}_k - \tilde{\mathbf{g}}_k, \quad (5)$$

where $\hat{\mathbf{g}}_k$ denotes the MMSE estimate of $\mathbf{g}_k$ with $\hat{\mathbf{g}}_k \sim \mathcal{CN}(\mathbf{0}, \gamma_k\mathbf{I}_M)$, where

$$\gamma_k = \mathbb{E}\left\{|\hat{g}_k^m|^2\right\} = \frac{\tau_{\mathrm{p}}\rho_u\beta_k^2}{\tau_{\mathrm{p}}\rho_u\beta_k + 1}, \quad (6)$$

while $\hat{g}_k^m$ is the m-th element of $\hat{\mathbf{g}}_k$; ρ_u represents the normalized signal-to-noise ratio (SNR) of each pilot symbol. Moreover, $\tilde{\mathbf{g}}_k \sim \mathcal{CN}\big(\mathbf{0}, (\beta_k - \gamma_k)\mathbf{I}_M\big)$ represents the channel estimation error vector. We notice that from the MMSE estimation property $\tilde{\mathbf{g}}_k$ is independent of $\hat{\mathbf{g}}_k$. We can represent the overall channel between the BS and users as

$$\hat{\mathbf{G}} = \mathbf{H}\mathbf{D}_\gamma^{\frac{1}{2}}, \quad (7)$$

where $\hat{\mathbf{G}} = [\hat{\mathbf{g}}_1, \ldots, \hat{\mathbf{g}}_K] \in \mathbb{C}^{M\times K}$; $\mathbf{H} = [\mathbf{h}_1, \ldots, \mathbf{h}_K] \in \mathbb{C}^{M\times K}$ with $\mathbf{h}_k \sim \mathcal{CN}(\mathbf{0}, \mathbf{I}_M)$; and $\mathbf{D}_\gamma = \mathrm{diag}\{\gamma_1, \ldots, \gamma_K\}$ is diagonal matrix. We can further represent $\hat{\mathbf{g}}_k$ as

$$\hat{\mathbf{g}}_k = \sqrt{\gamma_k}\mathbf{h}_k. \quad (8)$$

2) Uplink training for MIMO Radar: let τ^{r} be the uplink training duration (in samples) per coherence interval During the training phase, radar simultaneously send pilot sequences of length τ^{r} samples to BS

$\sqrt{\tau^{\mathrm{r}}}\boldsymbol{\varphi}_r$ is $\in \mathbb{C}^{\tau^{\mathrm{r}}\times N}$, where $\|\boldsymbol{\varphi}_r\|^2 = 1$, be the pilot sequence used by the radar. The received pilot signal at the BS can be defined as:

$$\mathbf{Y}_{\mathrm{R}} = \sqrt{\tau^{\mathrm{r}}P_R}\mathbf{R}\boldsymbol{\varphi}_r^H + \sqrt{\tau^{\mathrm{p}}\rho_{ul}}\mathbf{G}\boldsymbol{\varphi}_p^H + \mathbf{N}, \quad (9)$$

Note (Pilot from users is orthogonal with pilot from radar, thus they cancel each other). where $\mathbf{N} \in \mathbb{C}^{M\times\tau^{\mathrm{r}}}$ Based on the received pilot signal the BS estimates the channel $\mathbf{R}$. Denote by $\check{\mathbf{Y}}_{\mathrm{R}}$ the projection of $\mathbf{Y}_{\mathrm{R}}$ onto $\boldsymbol{\varphi}_r$

$$\begin{aligned}\check{\mathbf{Y}}_{\mathrm{R}} &= \mathbf{Y}_{\mathrm{R}}\boldsymbol{\varphi}_r \\ &= \sqrt{\tau^{\mathrm{r}}P_R}\mathbf{R}\boldsymbol{\varphi}_r^H\boldsymbol{\varphi}_r + \mathbf{N}\boldsymbol{\varphi}_r \\ &= \sqrt{\tau^{\mathrm{r}}P_R}\mathbf{R}\mathbf{I}_N + \mathbf{N}_r \end{aligned} \quad (10)$$

where $\mathbf{N}_r = \mathbf{N}\boldsymbol{\varphi}_r$. By stacking all columns of $\check{\mathbf{Y}}_{\mathrm{R}}$ on top of each other, where vec(.) is the vectorization operation, we have

$$\mathrm{vec}\left(\check{\mathbf{Y}}_{\mathrm{R}}\right) = \sqrt{\tau^{\mathrm{r}}P_R}\mathrm{vec}\left(\mathbf{R}\right)\mathbf{I}_N + \mathrm{vec}\left(\mathbf{N}_r\right) \quad (11)$$

The MMSE estimate of R given $\check{\mathbf{Y}}_R$ is

$$\mathrm{vec}\left(\hat{\mathbf{R}}\right) = \frac{\mathbb{E}\left\{\mathrm{vec}\left(\check{\mathbf{Y}}_{\mathrm{R}}\right)\mathrm{vec}\left(\hat{\mathbf{R}}^{\mathbf{H}}\right)\right\}}{\mathbb{E}\left\{\left|\mathrm{vec}\left(\check{\mathbf{Y}}_{\mathrm{R}}\right)\right|^2\right\}}\mathrm{vec}\left(\check{\mathbf{Y}}_{\mathrm{R}}\right), \quad (12)$$

$$\mathrm{vec}\left(\hat{\mathbf{R}}\right) = \frac{\sqrt{\tau_{\mathrm{p}}P_R}\beta_{br}}{\tau_{\mathrm{p}}P_R\beta_{br}+1}\mathrm{vec}\left(\check{\mathbf{Y}}_{\mathrm{R}}\right) \quad (13)$$

The mean-square of the channel estimate is denoted by γ_r and given by

$$\gamma_r = \frac{\tau_{\mathrm{p}}P_R\beta_{br}^2}{\tau_{\mathrm{p}}P_R\beta_{br}+1} \quad (14)$$

3) Downlink transmission: After the training phase, the channel estimates are employed to precode the symbols for each user before the downlink transmission. Let d_k is the symbol intended for the k-th user. Assuming $E\left\{|d_k|^2\right\} = 1$, where the signal transmitted from the BS can be constructed as

$$\begin{aligned}\boldsymbol{x} &= \mathbf{T}\mathbf{D}_{\eta}^{\frac{1}{2}}\mathbf{d}\\ &= \sum_{k=1}^{K}\mathbf{t}_k\sqrt{\eta_k}\mathbf{d}_k,\end{aligned} \quad (15)$$

where $\mathbf{T}$ is the precoding matrix which is the function of the channel estimate $\hat{\mathbf{G}} = [\hat{\mathbf{g}}_1,\ldots,\hat{\mathbf{g}}_K]$, and $\mathbf{D}_{\eta}^{\frac{1}{2}}$ is diagonal matrix whose k-th diagonal element is denoted by η_k representing power control coefficients chosen to satisfy the power constraint at $\mathbb{E}\{\|\mathbf{x}\|^2\} \leq 1$ where $\sum_{k=1}^{K}\eta_k \leq 1$.

Then the received signal vector can be expressed as

$$\boldsymbol{y} = \underbrace{\sqrt{\rho}\boldsymbol{G}^{\mathrm{T}}\boldsymbol{x}}_{\text{desired signal}} + \underbrace{\sqrt{P_R}\mathbf{F}^T\mathbf{s}}_{\text{interference from radar}}, \quad +\boldsymbol{n} \quad (16)$$

where $\rho, P_R, \mathbf{F} \in \mathbb{C}^{N_t\times K}, \boldsymbol{n} \sim \mathcal{CN}\left(0,\sigma_C^2\right)$ and $\mathbf{S}$ denote the normalized signal-to-noise ratio (SNR), the transmitted power for MIMO radar, the interference channel matrix from radar to the k−th users, the received noise and $\mathbf{S} = [\mathbf{s}_1,\mathbf{s}_2,\ldots,\mathbf{s}_L] \in \mathbb{C}^{N_t\times L}$ is the transmitted wave forms for radar at the l-th snapshot across the transmit antennas respectively.

III. Performance Analysis

We evaluate the performance, in terms of downlink spectral efficiency (SE) [bit/s/Hz/user] and probability of detection, provided by coexistence of Massive MIMO communication and MIMO radar system, modeled as described in Section II, for different precoding schemes. In this section, imperfect CSI is used to implement all schemes considered and proposed.

A. Spectral Efficiency

The spectral efficiency at the k-th user is defined as

$$\mathrm{SE}_k = \log_2(1+\mathrm{SINR}_k). \quad (17)$$

In what follows we derive SINR_k by using the use-and-then-forget bounding technique [1, Eq. (2.44)] and for linear precoding MR, ZF, and PZF processing

1) Maximum-ratio transmission: The precoding matrix for MR can be defined as

$$\mathbf{T}^{\mathrm{MR}} = \frac{1}{\sqrt{M}}\mathbf{H}^*, \quad (18)$$

Then the received SINR at the k−th user using MR precoding is given by

Proposition 1:

$$\mathrm{SINR}_k^{\mathrm{MR}} = \frac{M\rho\gamma_k\eta_k}{\rho\beta_k\sum_{k'=1,}^{K}\eta_{k'} + P_R\bar{\beta}_kN_t + \sigma_C^2}. \quad (19)$$

Proof: See Appendix VI-A. ■

2) Zero forcing: The precoding matrix for ZF is given by

$$\mathbf{T}^{\mathrm{ZF}} = \sqrt{M-K}\mathbf{H}^*(\mathbf{H}^T\mathbf{H}^*)^{-1}. \quad (20)$$

Then the received SINR at the k−th user using ZF precoding is given by

Proposition 2:

$$\mathrm{SINR}_k^{\mathrm{ZF}} = \frac{(M-K)\rho\gamma_k\eta_k}{\rho(\beta_k-\gamma_k)\sum_{k'=1,k\neq k'}^{K}\eta_{k'} + P_R\bar{\beta}_kN_t + \sigma_C^2}. \quad (21)$$

Proof: See Appendix VI-B. ■

3) Protective Zero-Forcing: The PZF scheme ensures that radar is fully protected from BS interference effects, let $\mathbf{B}$ represents the projection matrix onto the orthogonal complement

$$\mathbf{B} = \mathbf{I}_M - \hat{\mathbf{R}}^*\left(\hat{\mathbf{R}}^T\hat{\mathbf{R}}^*\right)^{-1}\hat{\mathbf{R}}^T \quad (22)$$

Under the assumption of independent Rayleigh fading channel, the normalization term PZF is given by

$$\mathbf{t}_k^{\mathrm{PZF}} = \frac{\mathbf{B}\mathbf{w}_k^{\mathrm{ZF}}}{\sqrt{\mathbf{E}\{\mathrm{tr}(\mathbf{w}_k^{\mathrm{ZF}}(\mathbf{w}_k^{\mathrm{ZF}})^H\mathbf{B}^H\mathbf{B})\}}} \quad (23)$$

where $\mathbf{w}_k^{\mathrm{ZF}}$ and $\mathbf{t}_k^{\mathrm{PZF}}$ are k-th column of $\mathbf{W}^{\mathrm{ZF}}$ and $\mathbf{T}^{\mathrm{PZF}}$ matrices, respectively, where $\mathbf{W}^{\mathrm{ZF}} = \mathbf{H}^*(\mathbf{H}^T\mathbf{H}^*)^{-1}$ and $\mathbf{T}^{\mathrm{PZF}} = \mathbf{B}\mathbf{W}^{\mathrm{ZF}}$.

where $\mathbf{B}^H\mathbf{B} = \mathbf{B} = \mathbf{I}_M - \hat{\mathbf{R}}^*\left(\hat{\mathbf{R}}^T\hat{\mathbf{R}}^*\right)^{-1}\hat{\mathbf{R}}^T$.

By using the law of large numbers, as $M \to \infty$ we obtain

$$\begin{aligned}&\frac{1}{M}\hat{\mathbf{R}}^T\hat{\mathbf{R}}^* \to \gamma_r\mathbf{I}_M\\ &\hat{\mathbf{R}}^T\hat{\mathbf{R}}^* \approx M\gamma_r\mathbf{I}_M\end{aligned} \quad (24)$$

then $\mathbf{B} \approx \mathbf{I}_M - \hat{\mathbf{R}}^* \frac{1}{M\gamma_r}\hat{\mathbf{R}}^{\mathbf{T}}$. Therefore $\mathbf{E}\{\mathbf{B}\}$ can be obtained as:

$$\begin{aligned}\mathbf{E}\{\mathbf{B}\} &\approx \mathbf{I}_M - \frac{1}{M\gamma_r}\mathbf{E}\{\ \hat{\mathbf{R}}^*\hat{\mathbf{R}}^{\mathbf{T}}\} \\ &= \mathbf{I}_M - \frac{N}{M}\mathbf{I}_M \\ &= \frac{M-N}{M}\mathbf{I}_M \end{aligned} \tag{25}$$

Then we have

$$\begin{aligned}\mathbf{t}_k^{\mathrm{PZF}} &= \frac{\mathbf{B}\mathbf{w}_k^{\mathrm{ZF}}}{\sqrt{\frac{M-N}{M}\mathbf{E}\left\{(\mathrm{tr}(\mathbf{H}^T\mathbf{H}^*)^{-1})\right\}}} \\ &= \frac{1}{\sqrt{\frac{(M-N)}{M(M-K)}}}\mathbf{B}\mathbf{w}_k^{\mathrm{ZF}} \\ &= \sqrt{\frac{M(M-K)}{(M-N)}}\mathbf{B}\mathbf{w}_k^{\mathrm{ZF}} \\ &= \alpha_{\mathrm{PZF}}\mathbf{B}\mathbf{w}_k^{\mathrm{ZF}} \end{aligned} \tag{26}$$

where $\alpha_{\mathrm{PZF}} = \sqrt{\frac{M(M-K)}{(M-N)}}$. Then the received SINR at the $k-$th user using PZF precoding is given by

Proposition 3:

$$\mathrm{SINR}_k^{\mathrm{PZF}} = \frac{(M-K)(M-N)/M\rho\gamma_k\eta_k}{\rho\alpha_{\mathrm{PZF}}^2\left(1-\frac{N}{M}\right)^2(\beta_k-\gamma_k)\sum_{k'=1}^{K}\eta_{k'} + \bar{\beta}_k P_R N + \sigma_c^2}. \tag{27}$$

Proof: See Appendix VI-B. ■

B. Probability of Detection

In this section, we derive the probability of detection for our system, under the Neyman-Pearson criterion, by using the Generalized Likelihood Ratio Test, the asymptotic probability of detection for radar P_d is given as [33]

$$P_d = 1 - \mathfrak{F}_{X_2^2(\mu)}\left(\mathfrak{F}_{X_2^2}^{-1}\left(1-P_{FA}\right)\right), \tag{28}$$

where P_{FA} is radar's probability of false alarm, $\mathfrak{F}_{X_2^2(\mu)}$ is the non-central chi-square Cumulative Distribution Function (CDF) with 2 Degrees of Freedom (DoF), $\mathfrak{F}_{X_2^2}^{-1}$ is the inverse function of chi-square CDF, the non-centrality parameter, μ, for X_2^2 is given by

$$\mu = |\alpha|^2 LP_R\mathrm{tr}\left(\mathbf{A}\mathbf{A}^H\left(\mathbf{R}^T\tilde{\mathbf{T}}\mathbf{D}_\eta\mathbf{R}^* + \sigma_R^2\mathbf{I}_N\right)^{-1}\right), \tag{29}$$

where $\mathbf{R}$ represents the interference channel matrix from the BS to the radar's receiver, where the elements of $\mathbf{R}$ are i.i.d. $\sim \mathcal{CN}(0,\beta_{br})$.

By using the law of large numbers, as $M \to \infty$ we obtain

$$\frac{1}{M}\mathbf{R}^T\tilde{\mathbf{T}}\mathbf{D}_\eta\mathbf{R}^* - \frac{\beta_{br}}{M}\mathrm{tr}(\mathbf{D}_\eta\tilde{\mathbf{T}})\mathbf{I}_N \overset{a.s.}{\to} 0. \tag{30}$$

where $\overset{a.s.}{\to}$ denotes the almost sure convergence, this implies that at large M, $\frac{1}{M}\mathbf{R}^T\mathbf{D}_\eta\tilde{\mathbf{T}}\mathbf{R}^*$ is very close to $\frac{\beta_{br}}{M}\mathrm{tr}\mathbf{D}_\eta(\tilde{\mathbf{T}})\mathbf{I}_N$. As a result, the non-centrality parameter μ given by (29) can be approximated by

$$\begin{aligned}\mu &\approx |\alpha|^2 LP_R\mathrm{tr}\left(\mathbf{A}\mathbf{A}^H\left(\beta_{br}\mathrm{tr}(\mathbf{D}_\eta\tilde{\mathbf{T}})\mathbf{I}_N + \sigma_R^2\mathbf{I}_N\right)^{-1}\right) \\ &= \frac{|\alpha|^2 LP_R\mathrm{tr}(\mathbf{A}\mathbf{A}^H)}{\beta_{br}\mathrm{tr}\left(\mathbf{D}_\eta\tilde{\mathbf{T}}\right) + \sigma_R^2}. \end{aligned} \tag{31}$$

1) Maximum Transmission Ratio:

$$\begin{aligned}\tilde{\mathbf{T}}^{\mathrm{MR}} &= \sum_{k=1}^{K}\mathbf{t}_k^{\mathrm{MR}}(\mathbf{t}_k^{\mathrm{MR}})^H = \mathbf{T}^{\mathrm{MR}}(\mathbf{T}^{\mathrm{MR}})^H \\ &= \frac{1}{M}(\mathbf{H}^*\mathbf{H}^T) \end{aligned} \tag{32}$$

we notice that $\frac{1}{M}\mathbf{H}^*\mathbf{H}^T \to \mathbf{I}_K$ for sufficiently large values of M. Therefore, using the fact that $\mathrm{tr}\left(\mathbf{D}_\eta\tilde{\mathbf{T}}^{\mathrm{MR}}\right) \approx \mathrm{tr}\left(\mathbf{D}_\eta\right) = \sum_{k=1}^{K}\eta_k$, we have

$$\mu^{\mathrm{MR}} \approx \frac{|\alpha|^2 LP_R\mathrm{tr}\left(\mathbf{A}\mathbf{A}^H\right)}{\beta_{br}\sum_{k=1}^{K}\eta_k + \sigma_R^2}. \tag{33}$$

2) Zero Forcing: Form (31) the non-centrality parameter μ forX_2^2 in case of ZF will be approximated by:

$$\mu^{\mathrm{ZF}} \approx \frac{|\alpha|^2 LP_R\mathrm{tr}\left(\mathbf{A}\mathbf{A}^H\right)}{\beta_{br}\mathrm{tr}(\mathbf{D}_\eta\tilde{\mathbf{T}}^{\mathrm{ZF}}) + \sigma_R^2}, \tag{34}$$

where $\tilde{\mathbf{T}}^{\mathrm{ZF}}$ defined as:

$$\begin{aligned}\tilde{\mathbf{T}}^{\mathrm{ZF}} &= \mathbf{T}^{ZF}(\mathbf{T}^{ZF})^H \\ &= (M-K)\mathbf{H}^*(\mathbf{H}^T\mathbf{H}^*)^{-1})(\mathbf{H}^*(\mathbf{H}^T\mathbf{H}^*)^{-1}))^H \\ &= (M-K)\mathbf{H}^*(\mathbf{H}^T\mathbf{H}^*)^{-1}(\mathbf{H}^T\mathbf{H}^*)^{-1}\mathbf{H}^T. \end{aligned} \tag{35}$$

To this end, by using (35), we get

$$\begin{aligned}\mathrm{tr}\left(\mathbf{D}_\eta\tilde{\mathbf{T}}^{ZF}\right) &= (M-K)\mathrm{tr}\left(\mathbf{D}_\eta(\mathbf{H}^T\mathbf{H}^*)^{-1}\right) \\ &\overset{(a)}{\approx} \frac{M-K}{M}\mathrm{tr}\left(\mathbf{D}_\eta\right) \\ &\overset{(a)}{=} \frac{M-K}{M}\sum_{k=1}^{K}\eta_k, \end{aligned} \tag{36}$$

where (a) follows from the fact that $(\mathbf{H}^T\mathbf{H}^*)^{-1} \approx \frac{1}{M}\mathrm{tr}\left(\mathbf{I}_K\right)$ and (b) holds since $\mathrm{tr}\left(\mathbf{D}_\eta\right) = \sum_{k=1}^{K}\eta_k$. Then, the non-centrality parameter μ^{ZF} can be approximated by:

$$\mu^{\mathrm{ZF}} \approx \frac{|\alpha|^2 LP_R\mathrm{tr}\left(\mathbf{A}\mathbf{A}^H\right)}{\frac{(M-K)}{M}\beta_{br}\sum_{k=1}^{K}\eta_k + \sigma_R^2}. \tag{37}$$

3) Protective Zero-Forcing: Form (26) $\tilde{\mathbf{T}}^{PZF}$ could be defined as

$$\mathbf{T}^{\mathrm{PZF}} = \sqrt{\frac{M(M-K)}{(M-N)}}\mathbf{B}\mathbf{W}^{ZF} \tag{38}$$

The non-centrality parameter μ for X_2^2 in case of PZF will be approximated by:

$$\mu^{\mathrm{PZF}} \approx \frac{|\alpha|^2 L P_R \mathrm{tr}(\mathbf{A}\mathbf{A}^H)}{\beta_{br}\mathrm{tr}(\mathbf{D}_\eta \tilde{\mathbf{T}}^{\mathrm{PZF}}) + \sigma_R^2}, \tag{39}$$

where $\tilde{\mathbf{T}}^{\mathrm{PZF}}$ defined as

$$\begin{aligned}\tilde{\mathbf{T}}^{\mathrm{PZF}} &= \mathbf{T}^{\mathrm{PZF}}(\mathbf{T}^{\mathrm{PZF}})^H \\ &= \frac{M(M-K)}{(M-N)}\mathbf{B}\mathbf{W}^{\mathrm{ZF}}(\mathbf{W}^{\mathrm{ZF}})^H\mathbf{B}^H.\end{aligned} \tag{40}$$

Therefore, $\mathrm{tr}(\mathbf{D}_\eta\tilde{\mathbf{T}}^{\mathrm{PZF}})$ can be obtained as

$$\begin{aligned}\mathrm{tr}(\mathbf{D}_\eta\tilde{\mathbf{T}}^{\mathrm{PZF}}) &= \frac{M(M-K)}{(M-N)}\mathrm{tr}(\mathbf{D}_\eta\mathbf{B}\mathbf{W}^{\mathrm{ZF}}(\mathbf{W}^{\mathrm{ZF}})^H\mathbf{B}^H) \\ &\overset{(a)}{=} \frac{M(M-K)}{(M-N)}\mathrm{tr}(\mathbf{D}_\eta\mathbf{W}^{\mathrm{ZF}}(\mathbf{W}^{\mathrm{ZF}})^H\mathbf{B}^H\mathbf{B}) \\ &\overset{(b)}{=} \frac{M(M-K)}{(M-N)}\mathrm{tr}(\mathbf{D}_\eta\mathbf{H}^*(\mathbf{H}^T\mathbf{H}^*)^{-1} \\ &\times(\mathbf{H}^*(\mathbf{H}^T\mathbf{H}^*)^{-1})^H\mathbf{B}) \\ &= \frac{M(M-K)}{(M-N)} \\ &\times \mathrm{tr}(\mathbf{D}_\eta\mathbf{H}^*(\mathbf{H}^T\mathbf{H}^*)^{-1}(\mathbf{H}^T\mathbf{H}^*)^{-1}\mathbf{H}^T\mathbf{B}).\end{aligned} \tag{41}$$

where we have exploited: in (a) $\mathrm{tr}(\mathbf{XY}) = \mathrm{tr}(\mathbf{YX})$, in (b) $\mathbf{B}\mathbf{B}^H = \mathbf{B}$.

Denote $\mathbf{C}$ as

$$\mathbf{C} = \mathbf{H}^*(\mathbf{H}^T\mathbf{H}^*)^{-1}(\mathbf{H}^T\mathbf{H}^*)^{-1}\mathbf{H}^T. \tag{42}$$

Then, by substituting (22) into (41), we get

$$\begin{aligned}\mathrm{tr}(\mathbf{D}_\eta\tilde{\mathbf{T}}^{PZF}) &= \mathrm{tr}(\mathbf{D}_\eta\mathbf{C} - \mathbf{D}_\eta\hat{\mathbf{R}}^*\left(\hat{\mathbf{R}}^T\hat{\mathbf{R}}\right)^{-1}\hat{\mathbf{R}}^T\mathbf{C}) \\ &= \underbrace{\mathrm{tr}(\mathbf{D}_\eta\mathbf{C})}_{\mathrm{T}_1} - \underbrace{\mathrm{tr}(\mathbf{D}_\eta\hat{\mathbf{R}}^*\left(\hat{\mathbf{R}}^T\hat{\mathbf{R}}\right)^{-1}\hat{\mathbf{R}}^T\mathbf{C})}_{\mathrm{T}_2}.\end{aligned} \tag{43}$$

For simplistic we divided (43) into two terms, for T_1 we have

$$\begin{aligned}T_1 &= \mathrm{tr}(\mathbf{D}_\eta\mathbf{H}^*(\mathbf{H}^T\mathbf{H}^*)^{-1}(\mathbf{H}^T\mathbf{H}^*)^{-1}\mathbf{H}^T) \\ &= \mathrm{tr}(\mathbf{D}_\eta(\mathbf{H}^T\mathbf{H}^*)^{-1}) \\ &\approx \frac{1}{M}\mathrm{tr}(\mathbf{D}_\eta\mathbf{I}_K) \\ &= \frac{1}{M}\sum_{k=1}^{K}\eta_k.\end{aligned} \tag{44}$$

Before proceeding to derive T_2, we notice that

$$\begin{aligned}\mathbf{C} &= \mathbf{H}^*(\mathbf{H}^T\mathbf{H}^*)^{-1}(\mathbf{H}^T\mathbf{H}^*)^{-1}\mathbf{H}^T \\ &\approx \mathbf{H}^*(M\mathbf{I}_K)^{-1}(M\mathbf{I}_K)^{-1}\mathbf{H}^T \\ &= \frac{1}{M^2}\mathbf{H}^*\mathbf{H}^T\end{aligned} \tag{45}$$

Therefore, we have

$$\begin{aligned}T_2 &= \mathrm{tr}\big(\mathbf{D}_\eta\hat{\mathbf{R}}^*\left(\hat{\mathbf{R}}^T\hat{\mathbf{R}}^*\right)^{-1}\hat{\mathbf{R}}^T\mathbf{C}\big) \\ &\approx \frac{1}{M^2}\mathrm{tr}(\mathbf{H}^T\mathbf{D}_\eta\hat{\mathbf{R}}^*\left(\hat{\mathbf{R}}^T\hat{\mathbf{R}}^*\right)^{-1}\hat{\mathbf{R}}^T\mathbf{H}^*)\end{aligned} \tag{46}$$

??By using the law of large number when as $M \to \infty$.

$$\begin{aligned}&\frac{\mathbf{H}^T(\mathbf{D}_\eta\hat{\mathbf{R}}^*\left(\hat{\mathbf{R}}^T\hat{\mathbf{R}}^*\right)^{-1}\hat{\mathbf{R}}^T)\mathbf{H}^*}{M} \\ &\overset{M\to\infty}{\to} \frac{\mathrm{tr}(\mathbf{D}_\eta\hat{\mathbf{R}}^*\left(\hat{\mathbf{R}}^T\hat{\mathbf{R}}^*\right)^{-1}\hat{\mathbf{R}}^T)}{M}\mathbf{I}_K\end{aligned} \tag{47}$$

???? then by substituting (47) into (46), we have

$$\begin{aligned}T_2 &\approx \frac{1}{M^2}\mathrm{tr}(\hat{\mathbf{R}}^*\left(\hat{\mathbf{R}}^T\hat{\mathbf{R}}\right)^{-1}\hat{\mathbf{R}}^T\mathbf{D}_\eta) \\ &\approx \frac{1}{M^2}\mathrm{tr}(\mathbf{D}_\eta) \\ &\approx \frac{1}{M^2}\sum_{k=1}^{K}\eta_k.\end{aligned} \tag{48}$$

Therefore

$$\mathrm{tr}(\mathbf{D}_\eta\tilde{\mathbf{T}}^{\mathrm{PZF}}) \approx \frac{1}{M}\left(1-\frac{1}{M}\right)\sum_{k=1}^{K}\eta_k. \tag{49}$$

To this end, by substituting (49) into (41) and then plugging the results into (39), we have

$$\mu^{\mathrm{PZF}} \approx \frac{|\alpha|^2 L P_R \mathrm{tr}\big(\mathbf{A}\mathbf{A}^H\big)}{\beta_{br}\frac{M-K}{(M-N)}\sum_{k=1}^{K}\eta_k(1-\frac{1}{M}) + \sigma_R^2}. \tag{50}$$

By generalised Marcum Q-function, P_d can be written as

$$P_d = Q_1\big(\sqrt{\mu}, \sqrt{C_{FA}}\big), \tag{51}$$

where $Q_1(\cdot,\cdot)$ is Marcum Q-function of order 1, C_{FA} is given by $C_{FA} = \mathfrak{F}_{x_2^2}^{-1}(1-P_{FA})$.

IV. Power Optimization

We aim at allocating the transmitted power for radar P_R and power control coefficients η_k at BS to maximize the probability of detection for MIMO radar, under the constraints on per user spectral efficiency and sum of

power control coefficients η_k for BS. More precisely, the optimization problem is mathematically described as:

$$(\mathbb{P}1): \quad \max_{P_R,\eta_k} \quad P_d \tag{52a}$$
$$\text{s.t.} \quad \mathrm{SE}_k \le \mathrm{SE}_{k,\mathrm{th}}, \ \forall k, \tag{52b}$$
$$0 \le P_R \le P_{R,max}, \tag{52c}$$
$$\sum_{k=1}^{K} \eta_k \le 1, \tag{52d}$$

Where $P_{R,max}$ is the maximum transmit power at MIMO radar and $\mathrm{SE}_{\mathrm{th}}$ is the minimum spectral efficiency required by the k-th user. The constraint (52d) makes sure that all the power control coefficients are positive. Next, we further rewrite $(\mathbb{P}1)$ as the following optimization problem

$$(\mathbb{P}2): \quad \max_{P_R,\eta_k} \quad \mu \tag{53a}$$
$$\text{s.t.} \quad \mathrm{SE}_k \le \mathrm{SE}_{k,\mathrm{th}}, \ \forall k, \tag{53b}$$
$$0 \le P_R \le P_{R,max}, \tag{53c}$$
$$\sum_{k=1}^{K} \eta_k \le 1, \tag{53d}$$

In this work, we consider three common linear processing techniques: MR, ZF, and PZF processing. By invoking (33), (37), and (50), we can rewrite the optimization problem $(\mathbb{P}2)$ as

$$(\mathbb{P}3): \quad \max_{P_R,\eta_k} \quad \frac{|\alpha|^2 L P_R \mathrm{tr}\left(\mathbf{A}\mathbf{A}^H\right)}{a_i \beta_{br} \sum_{k=1}^{K} \eta_k + \sigma_R^2} \tag{54a}$$
$$\text{s.t.} \quad \frac{b_i \rho \eta_k \gamma_k}{\rho c_{i,k} \sum_{k'=1}^{K} \eta_{k'} + \bar{\beta}_k P_R N + 1} \ge \gamma_{k,\mathrm{th}}, \ \forall k, \tag{54b}$$
$$0 \le P_R \le P_{R,max}, \tag{54c}$$
$$\sum_{k=1}^{K} \eta_k \le 1, \tag{54d}$$

where $\gamma_{k,\mathrm{th}} = 2^{\mathrm{SE}_{k,\mathrm{th}}} - 1$, $i \in \{\mathrm{MR}, \mathrm{PZF}, \mathrm{ZF}\}$ and $a_{\mathrm{MR}} = 1$, $a_{\mathrm{PZF}} = \frac{M-K}{(M-N)}\left(1 - \frac{1}{M}\right)$, $a_{\mathrm{ZF}} = \frac{(M-K)}{M}$, $b_{\mathrm{MR}} = M$; $b_{\mathrm{PZF}} = \frac{1}{M}(M-K)(M-N)$, $b_{\mathrm{ZF}} = (M-K)$; $c_{\mathrm{MR},k} = \beta_k$, $c_{\mathrm{PZF},k} = b_{\mathrm{PZF}}(\beta_k - \gamma_k)$, and $c_{\mathrm{ZF},k} = \beta_k - \gamma_k$.

Since expression (54a) is quasi-concave, the optimisation problem is quasi-concave. Thus, problem $(\mathbb{P}3)$ can be equivalently reformulated as

$$(\mathbb{P}4): \quad \max_{P_R,\eta_k} \quad t \tag{55a}$$
$$\text{s.t.} \quad b_i \rho \eta_k \gamma_k \ge \gamma_{k,\mathrm{th}}\Big(\rho c_{i,k} \sum_{k'=1}^{K} \eta_{k'} + \bar{\beta}_k P_R N + 1\Big), \forall k, \tag{55b}$$
$$|\alpha|^2 L P_R \mathrm{tr}\left(\mathbf{A}\mathbf{A}^H\right) \ge t\Big(a_i \beta_{br} \sum_{k=1}^{K} \eta_k + \sigma_R^2\Big) \tag{55c}$$
$$0 \le P_R \le P_{R,max}, \tag{55d}$$
$$\sum_{k=1}^{K} \eta_k \le 1, \tag{55e}$$

where

$$t = \frac{|\alpha|^2 L P_R \mathrm{tr}\left(\mathbf{A}\mathbf{A}^H\right)}{a_i \beta_{br} \sum_{k=1}^{K} \eta_k + \sigma_R^2}. \tag{56}$$

Problems (55) can be solved efficiently by a bisection search, in each step solving a sequence of convex feasibility problems [34] as detailed in Algorithm 1.

Algorithm 1 Bisection Algorithm for Solving $(\mathbb{P}4)$

1: Initialization: choose the initial values of t_{min} and t_{max}, where t_{min} and t_{max} define a range of relevant values of the objective function, Choose a tolerance $\varsigma > 0$.
2: While $t_{min} - t_{max} < \varsigma$
3: Set $t = \frac{t_{min}+t_{max}}{2}$ and solve the feasibility problem.
4: If problems $(\mathbb{P}4)$ is feasible, then set $t_{min} = t$, else set $t_{max} = t$.
5: Stop if $t_{max} - t_{min} < \varsigma$. Otherwise, go to Step 2.

V. Numerical results

In this section, we provide numerical results to verify our analysis. We assume that the MIMO radar system deploys a ULA. The inter-antenna spacing for MIMO radar is $d = \lambda/2$. The radar SNR is defined as $SNR_R = \frac{L|\alpha|^2 P_R}{\sigma_R^2}$ [23]. The target is set to be located at the direction of $\theta = 10°$. In the next scenario, we have considered the more practical scenario where path loss, shadow fading, and random user locations are modeled to model large-scale fading. For generating large-scale fading $\beta_k, \bar{\beta}_k$ and β_{br}, we follow model as in [35]. For a better understanding, let us consider a circular cell with a radius of ** Km. In the centre of the cell, there is a BS with M antennas serving K users that are randomly located within this cell. The MIMO radar is located 2 Km from

$$\mathrm{SE}_k^{\mathrm{MR}} = \log_2\left(1 + \frac{M\rho\eta_k\gamma_k}{\rho\beta_k\sum_{k'=1}^{K}\eta_{k'} + \bar{\beta}_k P_R N + \sigma_c^2}\right), \forall k \tag{57}$$

$$\mathrm{SE}_k^{\mathrm{ZF}} = \log_2\left(1 + \frac{(M-K)\rho\gamma_k\eta_k}{\rho(\beta_k-\gamma_k)\sum_{k'=1}^{K}\eta_{k'} + \bar{\beta}_k P_R N + \sigma_c^2}\right), \forall k. \tag{58}$$

$$\mathrm{SE}_k^{\mathrm{PZF}} = \log_2\left(1 + \frac{\frac{\rho}{M}(M-K)(M-N)\gamma_k\eta_k}{\frac{\rho}{M}(M-N)(M-K)(\beta_k-\gamma_k)\sum_{k'=1}^{K}\eta_{k'} + \bar{\beta}_k P_R N + \sigma_c^2}\right), \forall k. \tag{59}$$

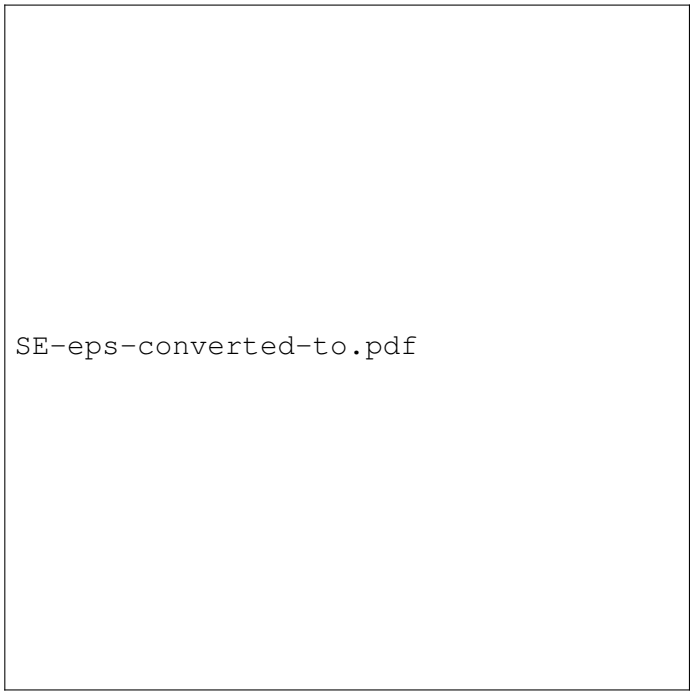

Fig. 2. SE versus number of base station antennas, M, (N = 20, K = 20, ρ = 10 dB).

Fig. 3. Spectral efficiency versus the number of users, for MR, ZF and PZF, (M = 100, ρ = 10 dB, N = 20).

the BS. The large-scale fading coefficient β_k is modeled as

$$\beta_k = \mathrm{PL}_0\left(\frac{d_k}{R_{\min}}\right)^{\upsilon} \times 10^{\frac{\sigma_{\mathrm{sh}}\cdot\mathcal{N}(0,1)}{10}}, \tag{61}$$

where d_k is the distance between user k and the MIMO radar, while $PL_0, \upsilon, \sigma_{\mathrm{sh}}$ denote a reference path loss constant which is chosen to satisfy a given downlink cell-edge SNR, path loss exponent and the standard deviation of the shadow fading, respectively. The same model is applied for $\bar{\beta}_k$ and β_{br}. In our examples, we chose υ = 3.8, σ_{sh} = 8dB, Fig. 2 shows the spectral efficiency Vs number of base station antennas for MR, ZF and PZF Fig. 4 shows that the probability of detection improves when the SNR increases, where M = 100, K = 40, N = 20 and ρ = 10 dB.

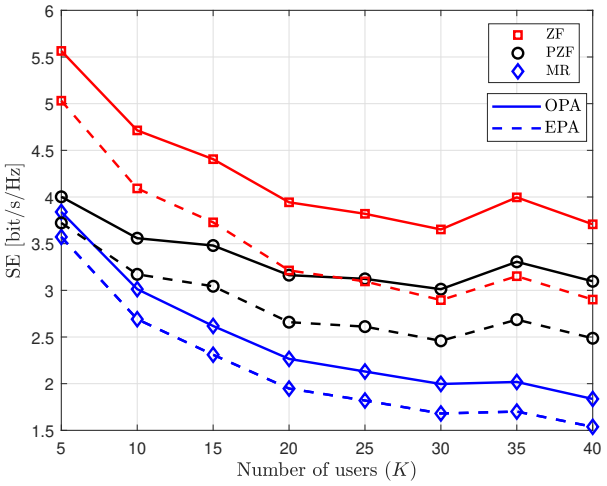

Fig. 4. Average detection probability versus the radar SNR, for MR, ZF and PZF (M = 100, K = 40, N = 20).

VI. Appendix

A. Proof of Proposition 1

For better presentation, I think you should move the first part of this Appendix (till before (71) to the main text after (16) and then represent the use-then-forget bounding in subsection III-A. By applying (5) into (16), the received signal vector is

$$\boldsymbol{y} = \sqrt{\rho}\hat{\mathbf{G}}^{\mathrm{T}}\boldsymbol{x} - \sqrt{\rho}\tilde{\mathbf{G}}^{\mathrm{T}}\boldsymbol{x} + \sqrt{P_R}\mathbf{F}^T\mathbf{s} + \boldsymbol{n} \tag{62}$$

The first term of (62) is the desired signal while the second term is the interference caused by the channel estimation error and the third term is the interference caused by radar. By applying(15) into (62) we obtain

$$\boldsymbol{y} = \sqrt{\rho}\hat{\mathbf{G}}^{\mathrm{T}}\mathbf{T}\mathbf{D}_\eta^{1/2}d - \sqrt{\rho}\tilde{\boldsymbol{G}}^{\mathrm{T}}\boldsymbol{x} + \sqrt{P_R}\mathbf{F}^T\mathbf{s} + \boldsymbol{n} \tag{63}$$

$$\begin{aligned}\boldsymbol{y} &= \sqrt{\frac{\rho}{M}}\hat{\boldsymbol{G}}^{\mathrm{T}}\mathbf{H}^*\mathbf{D}_\eta^{1/2}d + -\sqrt{\rho}\tilde{\boldsymbol{G}}^{\mathrm{T}}\boldsymbol{x} + \sqrt{P_R}\mathbf{F}^T\mathbf{s} + \boldsymbol{n} \\ &= \sqrt{\frac{\rho}{M}}\mathbf{D}_\gamma^{1/2}\boldsymbol{H}^{\mathrm{T}}\mathbf{H}^*\mathbf{D}_\eta^{1/2}d - \sqrt{\rho}\tilde{\boldsymbol{G}}^{\mathrm{T}}\boldsymbol{x} + \sqrt{P_R}\mathbf{F}^T\mathbf{s} + \boldsymbol{n}\end{aligned} \tag{64}$$

The equation (64) can be further expressed as

$$\begin{aligned}\boldsymbol{y} = &\sqrt{\frac{\rho}{M}}\mathbf{D}_\gamma^{1/2}\mathrm{E}\left\{\mathbf{H}^{\mathrm{T}}\mathbf{H}^*\right\}\mathbf{D}_\eta^{1/2}d - \sqrt{\rho}\tilde{\boldsymbol{G}}^{\mathrm{T}}\boldsymbol{x} \\ &+ \sqrt{\frac{\rho}{M}}\mathbf{D}_\gamma^{1/2}\left(\mathbf{H}^{\mathrm{T}}\mathbf{H}^* - \mathrm{E}\left\{\mathbf{H}^{\mathrm{T}}\mathbf{H}^*\right\}\right)\mathbf{D}_\eta^{1/2}\boldsymbol{q} \\ &+ \sqrt{P_R}\mathbf{F}^T\mathbf{s} + \boldsymbol{n}.\end{aligned} \tag{65}$$

Then (65) is simplified as (66) at the top of the next page. This is actually the received signal at the k-th users and not a simplified version. According to definition of $\mathbf{H}$ in (7), you need to replace $\mathbf{H}_k$ ($\mathbf{H}_{k'}$) with $\mathbf{h}_k$ ($\mathbf{h}_{k'}$). The first term is treated as the desired part of the received signal and the rest are treated as noise in the signal detection. More precisely, we utilize the use-and-then-forget technique.

The first term represents the desired signal.

$$\frac{\rho\eta_k\gamma_k}{M}\left(\mathbb{E}\left\{\|\mathbf{H}_k\|^2\right\}\right)^2 = M\rho\gamma_k\eta_k \tag{71}$$

The second term represents noise and channel estimation errors

$$\begin{aligned}\mathrm{E}\left\{\sqrt{\rho}\widetilde{\boldsymbol{g}}_k^{\mathrm{T}}\boldsymbol{x}\right\} &= \rho\mathrm{E}\left\{\boldsymbol{x}^{\mathrm{H}}\widetilde{\boldsymbol{g}}_k^*\widetilde{\boldsymbol{g}}_k^{\mathrm{T}}\boldsymbol{x}\right\} \\ &= \rho\left(\beta_k - \gamma_k\right)\end{aligned} \tag{72}$$

The third term represents channel non-orthogonality

$$\frac{\rho\gamma_k}{M}\mathrm{Var}\left\{\sum_{k'=1,k\neq k'}^{K}\sqrt{\eta_{k'}}\mathbf{h}_k^T\mathbf{H}_{k'}^*d_{k'}\right\} = \rho\gamma_k\sum_{k'=1,k\neq k'}^{K}\eta_{k'} \tag{73}$$

The fourth term represents beamforming gain uncertainty which has variance,

$$\frac{\rho\gamma_k\eta_k}{M}\mathrm{Var}\left\{\left(\|\mathbf{H}_k\|^2 - \mathrm{E}\left\{\|\mathbf{H}_k\|^2\right\}\right)d_k\right\} = \rho\gamma_k\eta_k. \tag{74}$$

The fifth term represents the radar's interference, assuming the channel between MIMO radar and the k-th users is Rayleigh fading, then

$$P_R\mathbb{E}\left\{\|\mathbf{f}_k^T\|^2\right\} = P_R\bar{\beta}_kN_t. \tag{75}$$

B. Proof of Proposition VI-B

By applying (20) into (16), we obtain the received signal

$$\begin{aligned}\mathbf{y} &= \sqrt{\rho(M-K)}\hat{\mathbf{G}}^T\mathbf{H}^*(\mathbf{H}^T\mathbf{H}^*)^{-1}\mathbf{D}_\eta^{\frac{1}{2}}\boldsymbol{d} \\ &\sqrt{\rho}\tilde{\mathbf{G}}^T\boldsymbol{x} + \sqrt{P_R}\mathbf{F}^T\mathbf{S} + \boldsymbol{n}_k \\ &= \sqrt{\rho(M-K)}\mathbf{D}_\gamma^{\frac{1}{2}}\mathbf{H}^T\mathbf{H}^*(\mathbf{H}^T\mathbf{H}^*)^{-1}\mathbf{D}_\eta^{\frac{1}{2}}\boldsymbol{d} \\ &\sqrt{\rho}\tilde{\mathbf{G}}^T\boldsymbol{x} + \sqrt{P_R}\mathbf{F}^T\mathbf{S} + \boldsymbol{n}_k \\ &= \sqrt{\rho(M-K)}\mathbf{D}_\gamma^{\frac{1}{2}}\mathbf{D}_\eta^{\frac{1}{2}}\boldsymbol{d} - \sqrt{\rho}\tilde{\mathbf{G}}^T\boldsymbol{x} + \sqrt{P_R}F^T\mathbf{S} + \boldsymbol{n}_k.\end{aligned} \tag{76}$$

Then, the received signal at the k-th user can be written as

$$y_k = \sqrt{(M-K)\rho\gamma_k\eta_k}d_k - \sqrt{\rho}\tilde{\mathbf{g}}_k^T\boldsymbol{x} + \sqrt{P_R}\mathbf{f}_k^T\mathbf{s}_l + \boldsymbol{n}_k. \tag{77}$$

The first term represents the desired signal.

$$\sqrt{(M-K)\rho\gamma_k\eta_k}d_k = (M-K)\rho\gamma_k\eta_k. \tag{78}$$

The second term represents

$$\begin{aligned}\sqrt{\rho}\tilde{\mathbf{g}}_k^T\boldsymbol{x} &= \rho\mathbf{E}\{\boldsymbol{x}^H\tilde{\mathbf{g}}_k^*\tilde{\mathbf{g}}_k^T\boldsymbol{x}\} \\ &= \rho(\beta_k - \gamma_k)\sum_{k'=1,k\neq k'}^{K}\eta_{k'}.\end{aligned} \tag{79}$$

The last term represents the radar's interference, assuming the channel between MIMO radar and the k-th users is Rayleigh fading, then

$$P_R\mathbb{E}\left\{\|\mathbf{f}_k^T\|^2\right\} = P_R\bar{\beta}_kN_t. \tag{80}$$

C. Proof of Proposition VI-C

The received signal at the k-th user can be expressed as

$$\begin{aligned}y_k = &\sqrt{\rho\eta_k}\mathbb{E}\left\{\mathbf{g}_k^T\mathbf{t}_k^{\mathrm{PZF}}\right\}d_k + \sqrt{\rho\eta_k}\left(\mathbf{g}_k^T\mathbf{t}_k^{\mathrm{PZF}} - \mathbb{E}\left\{\mathbf{g}_k^T\mathbf{t}_k^{\mathrm{PZF}}\right\}\right)d_k \\ &+ \sqrt{\rho\eta_k}\sum_{j=1,j\neq k}^{K}\mathbf{g}_k^T\mathbf{t}_j^{\mathrm{PZF}}d_j + P_R\mathbb{E}\{\|\mathbf{f}_k\|^2\} + n_k.\end{aligned} \tag{81}$$

$$
\begin{aligned}
y_k &= \sqrt{\frac{\rho\gamma_k}{M}}\mathrm{E}\left\{\mathbf{H}_k^{\mathrm{T}}\boldsymbol{H}^*\right\}\boldsymbol{D}_\eta^{1/2}d - \sqrt{\rho}\tilde{\mathbf{g}}_k^{\mathrm{T}}\boldsymbol{x} + \sqrt{\frac{\rho\gamma_k}{M}}\left(\mathbf{H}_k^{\mathrm{T}}\boldsymbol{H}^* - \mathrm{E}\left\{\mathbf{H}_k^{\mathrm{T}}\boldsymbol{H}^*\right\}\right)\boldsymbol{D}_\eta^{1/2}\boldsymbol{d} + \sqrt{P_R}\mathbf{f}_k^T\mathbf{s}_l + n_k \\
&= \sqrt{\frac{\rho\gamma_k\eta_k}{M}}\mathrm{E}\left\{\|\mathbf{H}_k\|^2\right\}d_k - \sqrt{\rho}\tilde{\boldsymbol{g}}_k^{\mathrm{T}}\boldsymbol{x} + \sqrt{\frac{\rho\gamma_k}{M}}\sum_{\substack{k'=1\\k'\neq k}}^{K}\sqrt{\eta_{k'}}\mathbf{H}_k^{\mathrm{T}}\mathbf{H}_{k'}^*d_{k'} \\
&+ \sqrt{\frac{\rho\gamma_k\eta_k}{M}}\left(\|\mathbf{H}_k\|^2 - \mathrm{E}\left\{\|\mathbf{H}_k\|^2\right\}\right)d_k + \sqrt{P_R}\mathbf{f}_k^T\mathbf{s}_l + \boldsymbol{n}_k. \qquad (66)
\end{aligned}
$$

The first term represents the desired signal.

$$
\begin{aligned}
\mathrm{DS}_k &= \sqrt{\rho\eta_k}\mathbb{E}\left\{(\hat{\mathbf{g}}_k^T - \tilde{\mathbf{g}}_k^T)\mathbf{t}_k^{\mathrm{PZF}}\right\} \\
&= \sqrt{\frac{\rho\eta_k M(M-K)}{M-N}}\mathbb{E}\left\{\hat{\mathbf{g}}_k^T\mathbf{B}\mathbf{w}_k^{\mathrm{ZF}}\right\} \\
&= \sqrt{\frac{\rho\eta_k\gamma_k M(M-K)}{M-N}}(\mathbb{E}\left\{\mathbf{h}_k^T\mathbb{E}\{\mathbf{B}\}\mathbf{w}_k^{\mathrm{ZF}}\right\}) \\
&= \sqrt{\frac{\rho\eta_k\gamma_k M(M-K)}{M-N}\frac{M-N}{M}}(\mathbb{E}\left\{\mathbf{h}_k^T\mathbf{w}_k^{\mathrm{ZF}}\right\}) \\
&= \sqrt{\frac{\rho\eta_k\gamma_k(M-K)(M-N)}{M}} \qquad (82)
\end{aligned}
$$

In order to derive $\mathbb{E}\{|\mathrm{BU}_k|^2\}$, which can be further expressed by

$$
\mathbb{E}\{|\mathrm{BU}_k|^2\} = \mathbb{E}\{|\mathbf{g}_k^T\mathbf{t}_k^{\mathrm{PZF}}|^2\} - |\mathrm{DS}_k|^2, \qquad (83)
$$

we need to obtain the first term in (83), which can be written as

$$
\begin{aligned}
&\sqrt{\rho\eta_k}\mathbb{E}\left\{|\mathbf{g}_k^T\mathbf{t}_k^{\mathrm{PZF}}|^2\right\} = \rho\eta_k\alpha_{\mathrm{PZF}}^2\left(\mathbb{E}\left\{|\mathbf{g}_k^T\mathbf{w}_k^{\mathrm{ZF}}|^2\right\}\right) \\
&= \rho\eta_k\alpha_{\mathrm{PZF}}^2\left(\mathbb{E}\left\{\mathbf{g}_k^T\mathbf{B}\mathbf{w}_k^{\mathrm{ZF}}(\mathbf{w}_k^{\mathrm{ZF}})^H\mathbf{B}^H\mathbf{g}_k^*\right\}\right) \qquad (84)
\end{aligned}
$$

Denote $\mathbf{V}_k = \mathbf{w}_k^{\mathrm{ZF}}(\mathbf{w}_k^{\mathrm{ZF}})^H$. Then, we have

$$
\begin{aligned}
&\rho\eta_k\alpha_{\mathrm{PZF}}^2(\mathbb{E}\left\{|\mathbf{g}_k^T\mathbf{w}_k^{\mathrm{ZF}}|^2\right\}) \\
&= \rho\eta_k\alpha_{\mathrm{PZF}}^2(\mathbb{E}\left\{\mathbf{g}_k^T\mathbf{B}\mathbf{V}\mathbf{B}^H\mathbf{g}_k^*\right\}) \\
&= \rho\eta_k\alpha_{\mathrm{PZF}}^2(\mathbb{E}\big\{\mathbf{g}_k^T(\mathbf{I}_M - \mathbf{R}^*(\mathbf{R}^T\mathbf{R}^*)^{-1}\mathbf{R}^T)\mathbf{V}_k \\
&\quad\times(\mathbf{I}_M - \mathbf{R}^*(\mathbf{R}^T\mathbf{R}^*)^{-1}\mathbf{R}^T)\mathbf{g}_k^*\big\}) \\
&= \rho\eta_k\alpha_{\mathrm{PZF}}^2(\mathbb{E}\big\{(\mathbf{g}_k^T\mathbf{V}_k - \mathbf{g}_k^T\mathbf{v}\mathbf{R}^*(\mathbf{R}^T\mathbf{R}^*)^{-1}\mathbf{R}^T) \\
&\quad\times(\mathbf{g}_k^* - \mathbf{R}^*(\mathbf{R}^T\mathbf{R}^*)^{-1}\mathbf{R}^T\mathbf{g}_k^*)\big\}) \\
&= \rho\eta_k\alpha_{\mathrm{PZF}}^2\Big(\mathbb{E}\big\{\mathbf{g}_k^T\mathbf{V}_k\mathbf{g}_k^* - \mathbf{g}_k^T\mathbf{V}_k\mathbf{R}^* \\
&\quad\times(\mathbf{R}^T\mathbf{R}^*)^{-1}\mathbf{R}^T\mathbf{g}_k^* - \mathbf{g}_k^T\mathbf{R}^*(\mathbf{R}^T\mathbf{R}^*)^{-1}\mathbf{R}^T\mathbf{g}_k^* \\
&\quad+\mathbf{g}_k^T\mathbf{R}^*(\mathbf{R}^T\mathbf{R}^*)^{-1}\mathbf{R}^T\mathbf{V}_k(\mathbf{R}^*(\mathbf{R}^T\mathbf{R}^*)^{-1}\mathbf{R}^*\mathbf{g}_k^*\big\}\Big) \\
&= \rho\eta_k\alpha_{\mathrm{PZF}}^2\Big(\mathbb{E}\big\{\mathbf{g}_k^T\mathbf{V}_k\mathbf{g}_k^* - 2\mathbf{g}_k^T\mathbf{V}_k \\
&\quad\times\mathbf{R}^*(\mathbf{R}^T\mathbf{R}^*)^{-1}\mathbf{R}^T\mathbf{g}_k^* \\
&\quad+\mathbf{g}_k^T\mathbf{R}^*(\mathbf{R}^T\mathbf{R}^*)^{-1}\mathbf{R}^T\mathbf{V}_k(\mathbf{R}^*(\mathbf{R}^T\mathbf{R}^*)^{-1}\mathbf{R}^*\mathbf{g}_k^*\big\}\Big) \\
&\overset{(a)}{=} \rho\eta_k\alpha_{\mathrm{PZF}}^2\Big(\mathbb{E}\big\{\mathbf{g}_k^T\mathbf{V}_k\mathbf{g}_k^*\big\} - 2\mathbb{E}\big\{\mathbf{g}_k^T\mathbf{V}_k \\
&\quad\times\mathbb{E}\big\{\mathbf{R}^*(\mathbf{R}^T\mathbf{R}^*)^{-1}\mathbf{R}^T\big\}\mathbf{g}_k^*\big\} \\
&\quad+\mathbb{E}\big\{\mathbf{g}_k^T\mathbb{E}\big\{\mathbf{R}^*(\mathbf{R}^T\mathbf{R}^*)^{-1}\mathbf{R}^T\mathbf{V}_k \\
&\quad\times(\mathbf{R}^*(\mathbf{R}^T\mathbf{R}^*)^{-1}\mathbf{R}^*\big\}\mathbf{g}_k^*\big\}\Big) \\
&\overset{(b)}{=} \rho\eta_k\alpha_{\mathrm{PZF}}^2\Big(\mathbb{E}\big\{\mathbf{g}_k^T\mathbf{V}_k\mathbf{g}_k^*\big\} - 2\frac{N}{M}\mathbb{E}\big\{\mathbf{g}_k^T\mathbf{V}_k\mathbf{g}_k^*\big\} \\
&+\left(\frac{N}{M}\right)^2\mathbb{E}\big\{\mathbf{g}_k^T\mathbf{V}_k\mathbf{g}_k^*\big\}\Big) \\
&= \rho\eta_k\alpha_{\mathrm{PZF}}^2\Big(1 - \frac{N}{M}\Big)^2\mathbb{E}\big\{\mathbf{g}_k^T\mathbf{V}_k\mathbf{g}_k^*\big\} \qquad (85)
\end{aligned}
$$

where (a) holds since $\mathbf{R}$ is independent from $\mathbf{g}_k$ and $\mathbf{V}_k$; (b) follows from the fact that $\mathbb{E}\left\{\mathbf{R}^*(\mathbf{R}^T\mathbf{R}^*)^{-1}\mathbf{R}^T\right\} = \frac{N}{M}$ and following from the fact that $\mathbb{E}\big\{\mathbf{g}_k^T\mathbf{V}_k\mathbf{g}_k^*\big\} = 1$.

Then, we need to derive $\mathbb{E}\big\{\mathbf{g}_k^T\mathbf{V}_k\mathbf{g}_k^*\big\}$, which can be obtained as

$$
\begin{aligned}
\mathbb{E}\big\{\mathbf{g}_k^T\mathbf{V}_k\mathbf{g}_k^*\big\} &= \mathbb{E}\big\{(\hat{\mathbf{g}}_k^T - \tilde{\mathbf{g}}_k^T)\mathbf{V}_k(\hat{\mathbf{g}}_k^* - \tilde{\mathbf{g}}_k^*)\big\} \\
&= \mathbb{E}\big\{(\hat{\mathbf{g}}_k^T\mathbf{V}_k\hat{\mathbf{g}}_k^* + \tilde{\mathbf{g}}_k^T\mathbf{V}_k\tilde{\mathbf{g}}_k^*)\big\} \\
&= \mathbb{E}\big\{\hat{\mathbf{g}}_k^T\mathbf{V}_k\hat{\mathbf{g}}_k^*\big\} + \mathbb{E}\big\{\tilde{\mathbf{g}}_k^T\mathbf{V}_k\tilde{\mathbf{g}}_k^*\big\} \\
&= 1 + (\beta_k - \gamma_k). \qquad (86)
\end{aligned}
$$

Then we have

$$\begin{aligned}\mathbb{E}\{|\mathrm{BU}_k|^2\} &= \mathbb{E}\{|\mathbf{g}_k^T\mathbf{t}_k^{PZF}|^2\} - |\mathrm{DS}_k|^2 \\ &= \rho\eta_k\alpha_{\mathrm{PZF}}^2\Big(1-\frac{N}{M}\Big)^2 + \rho\eta_k\alpha_{\mathrm{PZF}}^2\Big(1-\frac{N}{M}\Big)^2(\beta_k-\gamma_k) \\ &\quad - \rho\eta_k\alpha_{\mathrm{PZF}}^2\Big(1-\frac{N}{M}\Big)^2 \\ &= \rho\eta_k\alpha_{\mathrm{PZF}}^2\Big(1-\frac{N}{M}\Big)^2(\beta_k-\gamma_k) \qquad (87)\end{aligned}$$

The third term (IUI) By using similar steps as in (85), we have

$$\begin{aligned}\rho\eta_{k'}\alpha_{\mathrm{PZF}}^2\mathbb{E}\left\{|\mathbf{g}_k^T\mathbf{B}\mathbf{w}_{k'}^{\mathrm{ZF}}|^2\right\} &= \rho\eta_{k'}\alpha_{\mathrm{PZF}}^2\Big(\mathbb{E}\big\{\mathbf{g}_k^T\mathbf{V}_{k'}\mathbf{g}_k^*\big\} \\ &\quad - 2\frac{N}{M}\mathbb{E}\big\{\mathbf{g}_k^T\mathbf{V}_{k'}\mathbf{g}_k^*\big\} + \left(\frac{N}{M}\right)^2 \\ &\quad \times \mathbb{E}\big\{\mathbf{g}_k^T\mathbf{V}_{k'}\mathbf{g}_k^*\big\}\Big) \\ &= \rho\eta_{k'}\alpha_{\mathrm{PZF}}^2\Big(1-\frac{N}{M}\Big)^2\mathbb{E}\big\{\mathbf{g}_k^T\mathbf{V}_k\mathbf{g}_k^*\big\} \qquad (88)\end{aligned}$$

Then for this term $\mathbb{E}\big\{\mathbf{g}_k^T\mathbf{V}_{k'}\mathbf{g}_k^*\big\} = \mathbb{E}\big\{(\hat{\mathbf{g}}_k^T-\tilde{\mathbf{g}}_k^T)\mathbf{V}_{k'}(\hat{\mathbf{g}}_k^*-\tilde{\mathbf{g}}_k^*)\big\}$

$$\begin{aligned}\mathbb{E}\big\{\mathbf{g}_k^T\mathbf{V}_{k'}\mathbf{g}_k^*\big\} &= \mathbb{E}\big\{(\hat{\mathbf{g}}_k^T-\tilde{\mathbf{g}}_k^T)\mathbf{V}_{k'}(\hat{\mathbf{g}}_k^*-\tilde{\mathbf{g}}_k^*)\big\} \\ &= \mathbb{E}\big\{(\hat{\mathbf{g}}_k^T\mathbf{V}_{k'}\hat{\mathbf{g}}_k^* + \tilde{\mathbf{g}}_k^T\mathbf{V}_{k'}\tilde{\mathbf{g}}_k^*)\big\} \\ &= \mathbb{E}\big\{\hat{\mathbf{g}}_k^T\mathbf{V}_{k'}\hat{\mathbf{g}}_k^*\big\} + \mathbb{E}\big\{\tilde{\mathbf{g}}_k^T\mathbf{V}_{k'}\tilde{\mathbf{g}}_k^*\big\} \\ &= 0 + (\beta_k-\gamma_k) \qquad (89)\end{aligned}$$

$$\rho\eta_{k'}\alpha_{\mathrm{PZF}}^2\mathbb{E}\left\{|\mathbf{g}_k^T\mathbf{B}\mathbf{w}_{k'}^{\mathrm{ZF}}|^2\right\} = \rho\eta_{k'}\alpha_{\mathrm{PZF}}^2\Big(1-\frac{N}{M}\Big)^2(\beta_k-\gamma_k) \qquad (90)$$

The forth term represents the radar's interference, assuming the channel between MIMO radar and the k-th users is Rayleigh fading, then

$$P_R\mathbb{E}\left\{\left\|\mathbf{f}_k^T\right\|^2\right\} = P_R\bar{\beta}_k N. \qquad (91)$$

REFERENCES

[1] T. L. Marzetta, *Fundamentals of massive MIMO*. Cambridge University Press, 2016.

[2] M. Matthaiou, O. Yurduseven, H. Q. Ngo, D. Morales-Jimenez, S. L. Cotton, and V. F. Fusco, "The road to 6G: Ten physical layer challenges for communications engineers," *IEEE Commun. Mag.*, vol. 59, no. 1, pp. 64–69, Jan. 2021.

[3] J. Zhang, E. Björnson, M. Matthaiou, D. W. K. Ng, H. Yang, and D. J. Love, "Prospective multiple antenna technologies for beyond 5G," *IEEE J. Sel. Areas Commun.*, vol. 38, no. 8, pp. 1637–1660, Aug. 2020.

[4] W. Saad, M. Bennis, and M. Chen, "A vision of 6G wireless systems: Applications, trends, technologies, and open research problems," *IEEE network*, vol. 34, no. 3, pp. 134–142, May/June 2019.

[5] statistic. (2022) connected-devices-worldwide. [Online]. Available: https://www.statista.com/statistics/1183457/iot-connected-devices-worldwide/

[6] L. Zheng, M. Lops, Y. C. Eldar, and X. Wang, "Radar and communication coexistence: An overview: A review of recent methods," *IEEE Signal Process. Mag.*, vol. 36, no. 5, pp. 85–99, Sept. 2019.

[7] F. Liu, C. Masouros, A. Petropulu, H. Griffiths, and L. Hanzo, "Joint radar and communication design: Applications, state-of-the-art, and the road ahead," *IEEE Trans. Commun.*, vol. 68, no. 6, pp. 3834–3862, Jun. 2020.

[8] Z. Zhang, Q. Chang, F. Liu, and S. Yang, "Dual-functional radar-communication waveform design: Interference reduction versus exploitation," *IEEE Commun. Lett.*, vol. 26, no. 1, pp. 148–152, Jan. 2021.

[9] J. Qian, M. Lops, L. Zheng, X. Wang, and Z. He, "Joint system design for coexistence of MIMO radar and MIMO communication," *IEEE Trans. Signal Process*, vol. 66, no. 13, pp. 3504–3519, Apr. 2018.

[10] F. Liu, A. Garcia-Rodriguez, C. Masouros, and G. Geraci, "Interfering channel estimation in radar-cellular coexistence: How much information do we need?" *IEEE Trans. Wireless Commun.*, vol. 18, no. 9, pp. 4238–4253, 2019.

[11] B. Li and A. P. Petropulu, "Joint transmit designs for coexistence of mimo wireless communications and sparse sensing radars in clutter," *IEEE Trans. Aerosp. Electron. Syst.*, vol. 53, no. 6, pp. 2846–2864, 2017.

[12] X. Wang, Z. Fei, J. Guo, Z. Zheng, and B. Li, "Ris-assisted spectrum sharing between MIMO radar and MU-MISO communication systems," *IEEE Wireless Commun. Lett.*, vol. 10, no. 3, pp. 594–598, Nov. 2020.

[13] M. Rihan and L. Huang, "Optimum co-design of spectrum sharing between mimo radar and mimo communication systems: An interference alignment approach," *EEE Trans. Veh. Technol.*, vol. 67, no. 12, pp. 11 667–11 680, Dec. 2018.

[14] F. Liu, C. Masouros, A. Li, H. Sun, and L. Hanzo, "MU-MIMO communications with mimo radar: From co-existence to joint transmission," *IEEE Trans Wireless Commun*, vol. 17, no. 4, pp. 2755–2770, 2018.

[15] Y. Li, L. Zheng, M. Lops, and X. Wang, "Interference removal for radar/communication co-existence: The random scattering case," *IEEE Trans. Wireless Commun.*, vol. 18, no. 10, pp. 4831–4845, Jul. 2019.

[16] K. Singh, S. Biswas, O. Taghizadeh, and T. Ratnarajah, "Beamforming design for coexistence of full-duplex multi-cell mu-mimo cellular network and mimo radar," in *Proc. IEEE Int. Conf. Acoust. Speech Signal Process. (ICASSP)*, May. 2019, pp. 7775–7779.

[17] E. Fishler, A. Haimovich, R. Blum, D. Chizhik, L. Cimini, and R. Valenzuela, "MIMO radar: An idea whose time has come," in *Proc. IEEE Radar Conf.*, Apr. 2004, pp. 71–78.

[18] X. Yu, G. Cui, T. Zhang, and L. Kong, "Constrained transmit beampattern design for colocated MIMO radar," *Signal Process*, vol. 144, pp. 145–154, Mar. 2018.

[19] J. Li and P. Stoica, "MIMO radar with colocated antennas," *IEEE Signal Process. Mag.*, vol. 24, no. 5, pp. 106–114, Sep. 2007.

[20] R. Saruthirathanaworakun, J. M. Peha, and L. M. Correia, "Opportunistic sharing between rotating radar and cellular," *IEEE J. Sel. Areas Commun.*, vol. 30, no. 10, pp. 1900–1910, Nov. 2012.

[21] F. Liu, C. Masouros, A. Li, T. Ratnarajah, and J. Zhou, "MIMO radar and cellular coexistence: A power-efficient approach enabled by interference exploitation," *IEEE Trans. Signal Process*, vol. 66, no. 14, pp. 3681–3695, May 2018.

[22] L. Wang, J. McGeehan, C. Williams, and A. Doufexi, "Application of cooperative sensing in radar–communications coexistence," *IET Commun.*, vol. 2, no. 6, pp. 856–868, 2008.

[23] F. Liu, C. Masouros, A. Li, and T. Ratnarajah, "Robust MIMO beamforming for cellular and radar coexistence," *IEEE Wireless Commun. Lett.*, vol. 6, no. 3, pp. 374–377, Apr. 2017.

[24] M. Alaee-Kerahroodi, E. Raei, S. Kumar, and B. S. M. R. Rao, "Coexistence of communications and cognitive MIMO radar: Waveform design and prototype," [Online]. Available https://arxiv.org/abs/2103.11890, 2021.

[25] H. Hua, J. Xu, and T. X. Han, "Optimal transmit beamforming for integrated sensing and communication," *arXiv preprint arXiv:2104.11871*, 2021.

[26] Y. He, Y. Cai, H. Mao, and G. Yu, "Ris-assisted communication radar coexistence: Joint beamforming design and analysis," *arXiv preprint arXiv:2201.07399*, 2022.

[27] C. D'Andrea, S. Buzzi, and M. Lops, "Communications and radar coexistence in the massive mimo regime: Uplink analysis," *IEEE Trans. Wireless Commun.*, vol. 19, no. 1, pp. 19–33, Jan. 2020.

[28] R. M. Rao, H. S. Dhillon, V. Marojevic, and J. H. Reed, "Underlay radar-massive mimo spectrum sharing: Modeling fundamentals and performance analysis," *IEEE Trans. Wireless Commun.*, vol. 20, no. 11, pp. 7213–7229, 2021.

[29] M. Alaee-Kerahroodi, K. V. Mishra, M. B. Shankar, and B. Ottersten, "Discrete-phase sequence design for coexistence of MIMO radar and MIMO communications," in *IEEE 20th Int. Workshop Signal Process. Adv. Wireless Commun. (SPAWC)*. IEEE, 2019, pp. 1–5.

[30] Z. Cheng, B. Liao, S. Shi, Z. He, and J. Li, "Co-design for overlaid MIMO radar and downlink MISO communication systems via cramér–rao bound minimization," *IEEE Trans. Signal Process.*, vol. 67, no. 24, pp. 6227–6240, Dec. 2019.

[31] J. A. Mahal, A. Khawar, A. Abdelhadi, and T. C. Clancy, "Spectral coexistence of MIMO radar and MIMO cellular system," *IEEE Trans. Aerosp. Electron. Syst.*, vol. 53, no. 2, pp. 655–668, Jan 2017.

[32] A. M. Ahmed, A. A. Ahmad, S. Fortunati, A. Sezgin, M. S. Greco, and F. Gini, "A reinforcement learning based approach for multitarget detection in massive MIMO radar," *IEEE Trans. Aerosp. Electron. Syst*, vol. 57, no. 5, pp. 2622–2636, Oct. 2021.

[33] S. András, A. Baricz, and Y. Sun, "The generalized Marcum $Q-$ function: an orthogonal polynomial approach," *Acta Univ. Sapientiae, Math.*, vol. 3, no. 5, pp. 60–76, Jan. 2010.

[34] S. Boyd, S. P. Boyd, and L. Vandenberghe, *Convex optimization*. Cambridge Univ. Press, 2004.

[35] H. Q. Ngo and E. G. Larsson, "No downlink pilots are needed in tdd massive MIMO," *IEEE Trans Wireless Commun*, vol. 16, no. 5, pp. 2921–2935, May 2017.